

#### 4.4 INVESTIGATION OF CARBON MONOXIDE TIME EVOLUTION OVER THE CITY OF SÃO PAULO DURING THE NIGHTTIME USING LES MODEL

Eduardo Barbaro\*, Amauri P. Oliveira, Jacyra Soares

Group of Micrometeorology, University of Sao Paulo, Sao Paulo, Brazil

### 1. INTRODUCTION

During the nighttime, even if the winds are weak, at few tenths of meters above the surface the wind frequently becomes super-geostrophic (Cuxart and Jiménez, 2006). This phenomenon is called low level jet (LLJ) and, at middle and higher latitudes, reaches its maximum intensity before the end of stable period. The LLJ is frequently located above the stable boundary layer (SBL) as result of the inertial oscillation of the flow aloft, which decouples from the surface as the surface temperature inversion intensifies (Blackadar, 1957). LLJ can also be generated by baroclinicity induced over sloped terrains or by land-sea thermal contrast (Karipot et al., 2008). The LLJ intensifies the vertical evolution of SBL and transports moisture and pollutants at regional scale (Wu and Raman, 1998).

Much progress has been made in describing the spatial and temporal evolution of the CBL, but the SBL has been less analyzed (Cederwall, 1994; Saiki et al., 2000; Kosovic and Curry, 2000; Beare et al., 2006 and van Dop and Axelsen, 2007).

Describing the behavior of the SBL faces additional difficulties when compared to the convective boundary layer (CBL) because when turbulence has low intensity several other processes, such as wave motions, baroclinicity, intermittency, radiational cooling compete with the turbulent mixing. In many situations, the non-turbulent processes increment the already large spatial and temporal variability of the SBL thermodynamic and dynamic properties (Galmarini et al., 1998; Saiki et al., 2000).

Facing all the limitations of measurements, numerical simulations are one the best alternative in the turbulence analysis. Nowadays, one of the most used numerical models to simulate the planetary boundary layer (PBL) is the Large-Eddy-Simulation (LES). In the last two decades the LES technique has been successfully used to simulate the PBL under convective and neutral conditions.

Only in the last decade LES model has been used to simulate the SBL more frequently. The main difficulty in simulating the SBL is that the eddy length scales are much smaller than in the CBL, requiring more spatial resolution, computational power and complex parameterizations for the sub-grid model (SGS), (Sullivan, 1994; Beare et al., 2006).

Despite the difficulties, the LES technique provides a very powerful tool to simulate dispersion of pollutants in the PBL. Sorbjan and Uliasz, 1999, used LES technique to study the effects of Stratocumulus clouds on the dispersion of contaminants in the SBL. Marques-Filho, 2006, used the LES model to describe the turbulent transport of a passive and inert pollutant over the CBL. Wang and Pitsch, 2007, used LES to analyze the mixing process of a cross-flow-jet combustion system in an industrial furnace and Karipot et al., 2008 proposed a study of the LLJ influence on the CO<sub>2</sub> flux measurements over a tall forest canopy.

The main objective of this work is to investigate the role played by the inversion layer and LLJ on the CO time evolution at the surface in the city of Sao Paulo, Brazil. In this paper two numerical experiments using LES technique are described: runs A and B. Run A is characterized by a weak geostrophic wind (5 ms<sup>-1</sup>) and run B by a strong geostrophic wind (10 ms<sup>-1</sup>). A detailed description about CO and wind evolutions at the surface will be presented in the section 2. Details about the numerical model and simulations A and B will be given at section 3. The results will be presented at section 4 and the main conclusions at section 5.

### 2. CO AND WIND AT THE SURFACE IN SÃO PAULO

The city of São Paulo, with about 11 million inhabitants, together with 39 other smaller cities, forms the Metropolitan Region of São Paulo (MRSP). This region, located about 60 km far from the Atlantic Ocean, is occupied by 20.5 millions of inhabitants and has approximately 7 million of vehicles. The MRSP has an area of 8,051 km<sup>2</sup> and it is considered the

---

\* *Corresponding author address:* Eduardo Barbaro, University of Sao Paulo, Group of Micrometeorology, Sao Paulo, Brazil. E-mail: [eduardo.barbaro@usp.br](mailto:eduardo.barbaro@usp.br)

largest conurbation in South America and one of the 10 largest in the world (Codato et al., 2008). The MRSP has emitted about 1,460,000 ton of carbon monoxide per year (CETESB, 2006). Approximately 97% of this emission is due to 7 million vehicles, and under low wind conditions a considerable fraction of carbon monoxide (CO) remains in the metropolitan area generating highly concentrations in the regions of intense traffic.

The observations of CO concentration displayed here in Fig. 1 and Fig. 2, (seasonal and diurnal evolution, respectively), were carried out by the air quality monitoring network of Sao Paulo State Environmental Protection Agency (CETESB, 2006) between 1996 and 2005 in the City of São Paulo.

The seasonal evolution indicates that the CO concentration in Sao Paulo presents a maximum of 2.45 ppm during winter (June) and a minimum of 1.56 ppm during summer (Fig. 1).

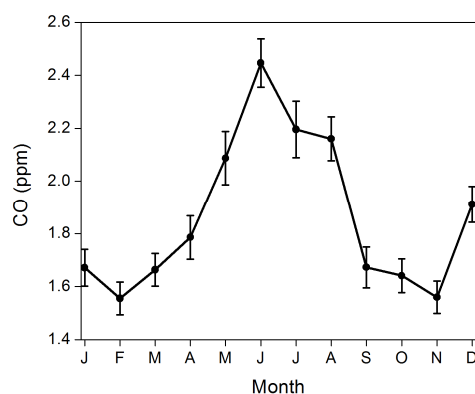


Fig. 1. Seasonal evolution of CO observed at the surface in the City of São Paulo between 1996 and 2005.

The Fig.2 shows the diurnal evolution of CO concentration at the surface in the city of São Paulo during June, the month with the highest CO concentration. There, the two well defined peaks that are mainly associated to the diurnal evolution of the traffic of vehicles in the MRSP can be visualized. The first peak occurs at 08:30 LT (2.90 ppm) and the second one at 20:30 LT (3.35 ppm). A minimum of 0.25 ppm takes place at 05:30 LT. The large nighttime variation of CO concentration at the surface (~ -3 ppm in 9 hours) is mainly related to the intense reduction in the vehicular emission. However, the presence of LLJ that frequently occurs over the MRSP area may contribute to strengthen or weaken this reduction of CO concentration at the surface during nighttime. This ventilation effect has been also observed to affect the concentration of pollutants at the surface (Cuxart and Jiménez, 2007) and minor atmospheric constituents

with source located at the surface (Karipot et al., 2008) in association to the presence of nocturnal LLJ.

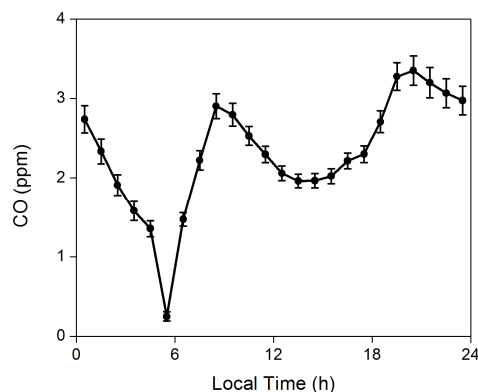


Fig. 2. Diurnal evolution of CO at the surface in the City of São Paulo observed during June between 1996 and 2005.

### 3. NUMERICAL MODEL

The LES model used here evaluates the explicitly the motion associated to large scale eddies and parameterize the small scale ones using a subgrid (SGS) model (Moeng, 1984; Moeng and Wyngaard, 1988; Sullivan, 1994).

The LES code used in this work was originally proposed by Moeng (1984) and improved by Sullivan et.al. (1994), mainly the 2-steps SGS scheme. The parallelized version was implemented in the cluster R900 Intel 2-quad (8 cores) 12 GB memory and 1.2 Tb HD.

#### 3.1 BOUNDARY AND INITIAL CONDITIONS

Two numerical experiments, hereafter called run A and run B, corresponding to geostrophic wind  $(U_g, V_g) = (5 \text{ ms}^{-1}, 0 \text{ ms}^{-1})$  and  $(U_g, V_g) = (10 \text{ ms}^{-1}, 0 \text{ ms}^{-1})$  respectively, were carried out to simulate 24 hours of PBL evolution, covering the convective and stable conditions. All the other initial and boundary conditions are the same in both simulations and they correspond to the typical condition observed in the city of São Paulo during winter, specifically in the month of June, when the atmospheric conditions do not favors the dispersion of pollutants and the concentration of CO is highest (Fig. 1).

The computations were carried out using a  $96^3$  evenly spaced grid points, distributed over domain of  $2 \times 2 \times 2 \text{ km}^3$ . The surface was considered flat and homogeneous landuse characterized by aerodynamic roughness of 0.1 m, corresponding to a typical urban area located in the city of São Paulo ( $23.34^\circ\text{S}$ ,  $46.44^\circ\text{W}$ ). The Coriolis parameter at this latitude is

$f = -0.57 \times 10^{-4} \text{ s}^{-1}$  and it corresponds to an inertial period of 30.62 hours.

The initial conditions (Fig. 3), in both simulations, consist of a weakly convective PBL with a variation of potential temperature between the surface (286 K) and the mixed layer equal to 1 K. The capping temperature inversion layer was set at 500 m, where the temperature inversion intensity increases 8 K over six  $\Delta z$  levels (125 m). The CO concentration difference between the surface (1.5 ppm) and mixed layer was set equal to 0.1 ppm. Above the mixed layer, the concentration of CO decreases 1 ppm over the same six  $\Delta z$  levels in the capping inversion layer. Above the inversion layer the potential temperature lapse-rate was set constant and equal to  $3 \text{ K km}^{-1}$  and the concentration of CO was set constant and equal to the pristine concentration in the region of São Paulo (0.4 ppm).

The initial wind profile was set constant over all the PBL and equal to the geostrophic value,  $(U_g, V_g) = [ (5 \text{ ms}^{-1}, 0 \text{ ms}^{-1}) \text{ and } (10 \text{ ms}^{-1}, 0 \text{ ms}^{-1}) ]$ , for run A and B, respectively (Fig. 4).

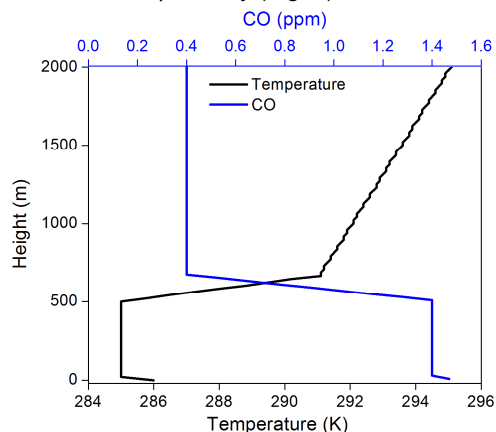


Fig. 3. Initial vertical profiles of potential temperature and concentration of CO. The profiles are equal in both simulations.

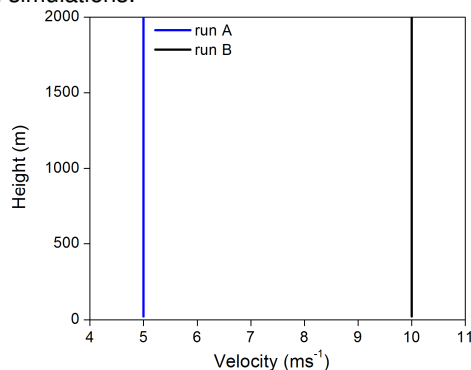


Fig.4. Vertical profiles of zonal components of the wind used as initial condition for run A and B. In both simulations the meridional components are set equal to zero.

To satisfy the CFL criteria, each simulation of 24 hours of PBL evolution used different time steps to take into consideration the differences in the geostrophic wind (Fig. 4). As consequence, the total CPU time used to simulate 24 hours of PBL evolution was about 19 hours for run A and 38 hours for run B. All simulations started at 6:30 LT.

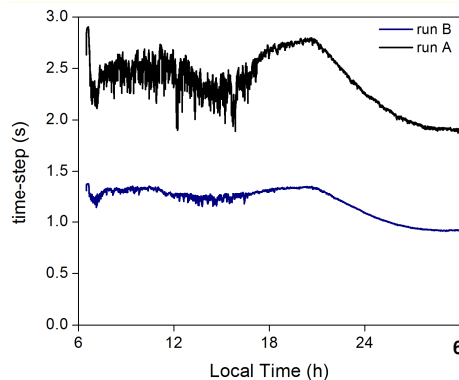


Fig. 5. Time step variation observed during run A and B.

Both simulations were carried out considering as input the time evolution of the potential temperature and concentration of CO observed in São Paulo in June (Codato et al., 2008). Figure 6 shows the time evolution of the potential temperature and concentration of CO used as the lower boundary conditions during the run A and B.

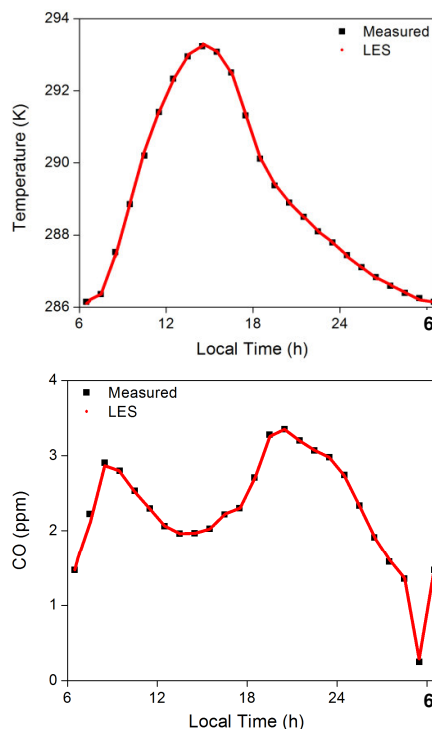


Fig. 6. Time evolution of potential temperature and CO concentration used as boundary conditions in the LES model. Red line indicates the linearly interpolated

values used at each time step. Black dots indicate the measured values in the City of São Paulo during June.

The continuous curve (LES) corresponds to linearly interpolated values at each time step (Fig. 5) between two consecutive hourly values (Measured).

#### 4. RESULTS

The results presented hereafter are based on statistics of the three-dimensional fields generated by LES model outputs (at each 100 time steps). Each set of output sample were separated by 1-2 minutes (on average). The statistical properties are estimated after PBL has reached a quasi-equilibrium state. According to Fig. 11 both simulations presented here reached quasi-equilibrium state after approximately 3000 seconds.

##### 4.1. Diurnal evolution of the PBL

Figure 7 describes the diurnal evolution of PBL height estimated as the level of the maximum vertical gradient of potential temperature. The PBL height is largest for run B during the convective (1240 m) and stable (275 m) periods. For run A, the PBL reaches 1088 m in the end of the convective period and 100 m in the end of the stable regime.

As expected, the highest PBL is associated to a more intense LLJ (run B) during the stable regime, (Fig. 8). The PBL height at nighttime is about 180% larger when the LLJ is higher (run B). For the convective conditions the relative differences between the PBL height of run B and A does not pass 20%. This pattern is controlled by the LLJ that intensifies the shear and the turbulent kinetic energy (TKE) production, (Figs 18, 19 and 20).

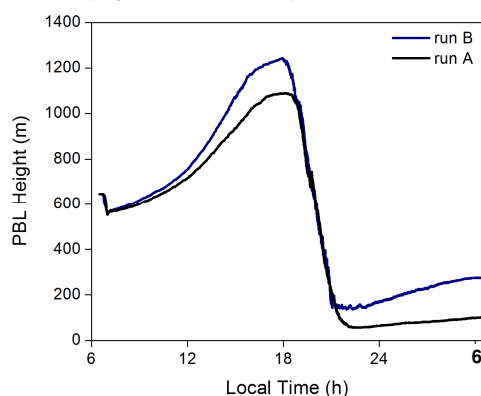


Fig. 7. Diurnal evolution of the PBL height for run A and B.

Therefore, the higher large scale wind forcing (given by geostrophic wind) provides enough wind shear to favor the growth of the PBL height either at convective and stable conditions.

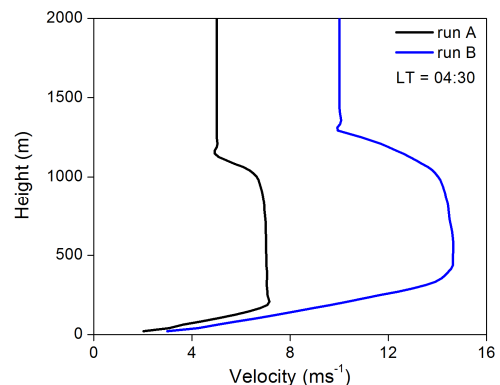


Fig. 8. Vertical profiles of wind speed at 04:30 LT for run A and B.

During the nighttime period, a large relative difference in the Obukhov length (Fig. 9) can be observed by comparing the simulations. The run B, with a more intense wind profile, shows  $L$  values 2-3 times greater than run A. This pattern is due to the differences in the LLJ intensity in both simulations, (Fig. 8).

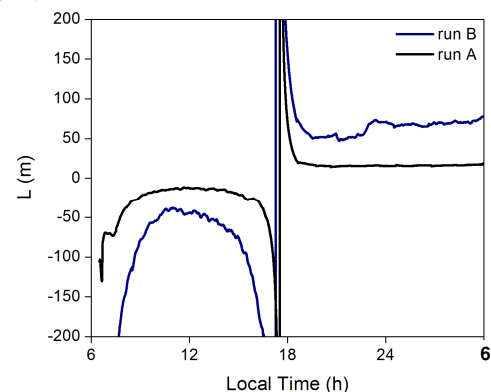


Fig. 9. Time evolution of Obukhov length,  $L$ , for run A and B.

The diurnal evolution of  $z_i/L$  indicates that In the case of weak geostrophic wind (run A) during the daytime period the turbulence in the PBL was highly convective with  $z_i/L$  reaching about -60 (Fig. 8). This is the typical condition observed in MRSP during the winter (Marques Filho et al. 2006; Codato et al, 2008). During nighttime, turbulence is strongly suppressed by the thermal stratification with  $z_i/L$  reaching about 60 (Fig. 10). For strong geostrophic wind (run B) the thermal convection and stratification are not so strong with  $Z_i/L$  reaching the values of about -20 and 20 respectively during daytime and nighttime.

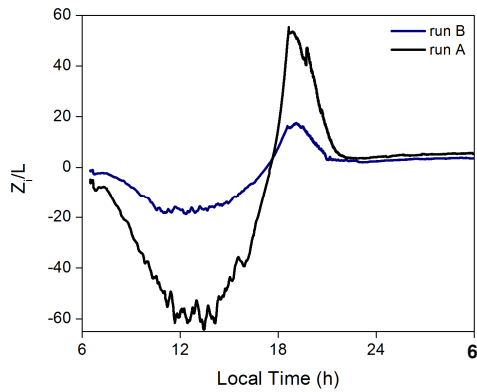


Fig. 10. Time evaluation of  $Z_i/L$  for run A and B.

The diurnal evolution of mean TKE in the PBL (Fig. 11) shows the expected behavior with a maximum at the end of the convective period and a minimum during nighttime. The onset of the LLJ for the case of stronger geostrophic wind (run B) can be identified by a local maximum around 22:00 LT.

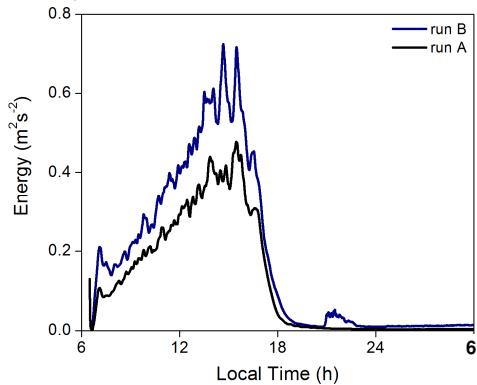


Fig. 11. Time evolution of mean TKE in the PBL.

Figure 12 describes the sensible heat flux at the surface. More intense LLJ is associated to large sensible heat flux and higher PBL height, at either night or daytime. The heat flux values presented here are representative of a winter period in the city of São Paulo (Ferreira, 2009).

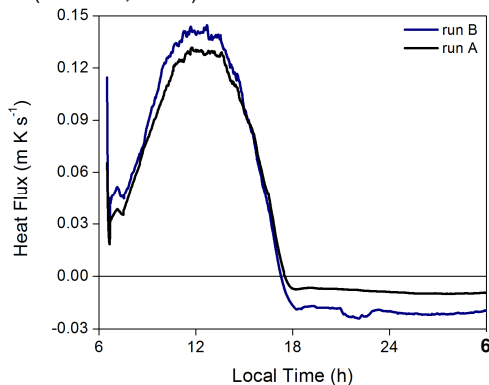


Fig. 12: Time evolution of sensible heat flux at the surface for run A and B.

The diurnal evolution of the simulated wind speed of run A compares well with observations in São Paulo during winter (Fig. 13). This agreement indicates that external forcing associated with the prescribed geostrophic wind in this case is more realistic and represent better the mean condition during June in MRSP. For run B, the simulated surface wind speed is more than twice of the observed values. Curiously, there is a local maximum at the end to convective period, around the middle of the afternoon, in both simulations (Fig. 13), that may be associated to the beginning of the inertial oscillation, when turbulence in the upper portions of the mixed layer starts to dies out.

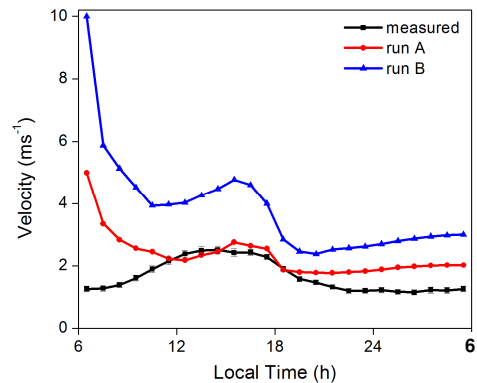


Fig. 13. Time evolution of the wind speed at the first level of the model (approximately 20m) for run A and run B. The observed wind speed in São Paulo is indicated by reference (at level 10 m).

Diurnal evolutions of the simulated vertical flux of CO at the surface show a bimodal character (Fig. 14). For comparison, the hypothetical diurnal evolution of CO flux estimated for the City of São Paulo from the vehicular emission inventory is also shown (Codato et al. 2008). During daytime, the simulated fluxes of CO in both cases match the estimated diurnal evolution of CO flux. Similar behavior occurs for the CO fluxes until around midnight. After that, the simulated CO fluxes become unrealistic negative. It is interesting to observe that regardless the time of the maximum, the LES model was able to simulate the amplitude of surface fluxes during most of the daytime and part of the nighttime period. Since, in the LES model the CO flux is estimated using the Monin-Obukhov Similarity Theory (MOST), assuming universal function for CO gradient is equal to the one for moisture. This assumption does not work after midnight, when vertical gradient of CO becomes positive and the CO flux turns into unrealistic negative. In the morning the CO flux matches well the CO flux estimated from diurnal evolution of vehicular traffic in São Paulo. However, in the afternoon, the position of the second peak of CO

flux (Fig. 14) is displaced. This feature is present in both simulations and may be related to the fact that when convection becomes less intense other non local effects, like horizontal advection of clean air associated to sea breeze penetration in São Paulo, become more important. Despite the discrepancy, the diurnal evolution of CO flux simulated by the LES model seems to reproduce the diurnal cycle based on the inventory of CO emitted annually in the city of São Paulo and on the diurnal evolution of the traffic of vehicles (Codato et al, 2008).

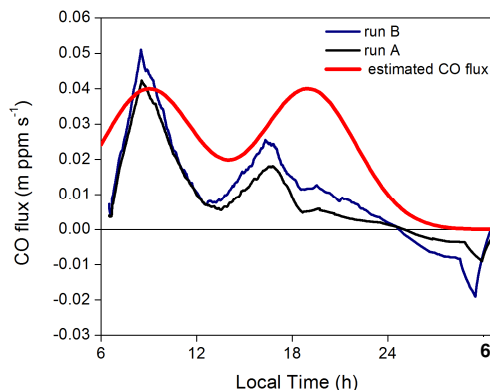


Fig.14. Time evolution of the vertical flux of CO in both simulations and estimated by CETESB inventory.

#### 4.2. Budget of the turbulent kinetic energy in the PBL

The vertical distributions of the components of TKE equation representative of the convective period are indicated in the figure 15. They correspond to the evolution of PBL simulated at 12:30 LT, time of the day when the sensible heat flux reaches the maximum value at the surface (Fig. 11).

According to the results shown in figure 15, one can observe that the vertical profile of the thermal production vary linear with height in both simulations. Buoyancy reaches a local minimum in the top of the PBL. The vertical profile of shear production varied significantly with intensity of large scale wind forcing. For run A, the shear is almost zero during all the PBL evolution because the wind forcing was weak. Shear production become more important in run B. In this case, the shear production is significantly in the first 200 m. In run A the shear production is significantly in the first 150 m.

The transport term, containing transport of TKE due to wind and pressure fluctuations, is negative in the lower portions of the PBL and becomes positive in the upper portions of the PBL. This pattern indicates that TKE is been removed from surface and transported to the top of PBL by the large eddies. The negative dissipation indicates that most

the turbulence generated by thermal and mechanical productions of TKE is removed by molecular dissipation throughout of the PBL.

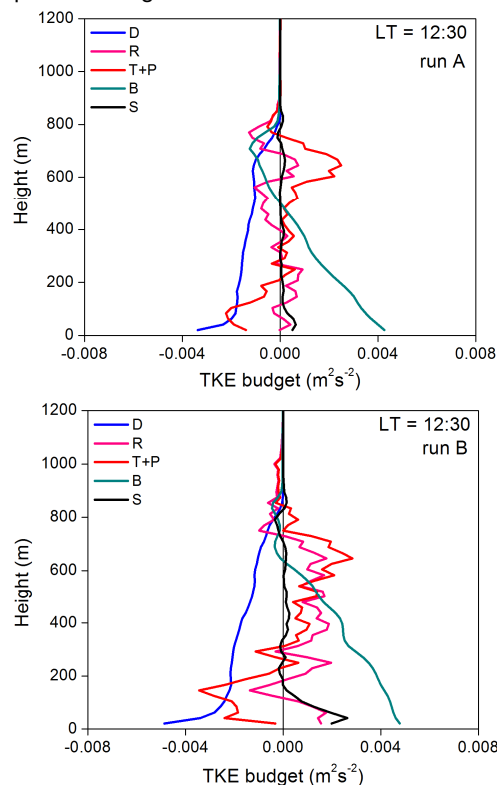


Fig.15. Vertical distribution of the components of TKE equation at 12:30 LT for run A and B. S indicates shear production, B buoyancy, T+P transport due to wind and pressure fluctuations, D molecular dissipation. The residues are indicated by R.

The vertical distributions of the TKE equation components, representative of the stable conditions, are indicated in the figures 16 and 17. The vertical profiles correspond to the evolution of the PBL at 00:30 LT and 04:30 LT, (moderate and strong LLJ intensity respectively).

The LLJ modulates the intensity of the TKE-equation components. The shear contribution is less intense for run A at 00:30 LT in comparison to run B at 04:30 LT. The thermal stratification associated with the buoyancy remove most of the TKE during the stable regime. Molecular dissipation appears to be important only for run B at 00:30 LT and 04:30 LT (Figs. 16 and 17) due to the large scale wind forcing. Molecular dissipation should be important regardless the height of the PBL. This apparent discrepancy may be associated to the sub-grid parameterization, that does not seems to handle dissipation properly for PBL heights below 100 meters in the simulations described here. A higher grid resolution would be necessary

needs to reduce the SGS contribution and improve the results in this case.

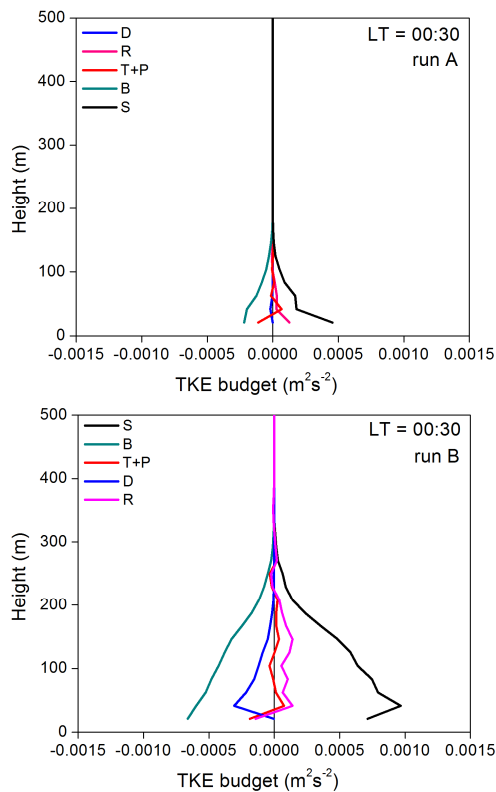


Fig.16. Idem to figure 15 for 00:30 LT.

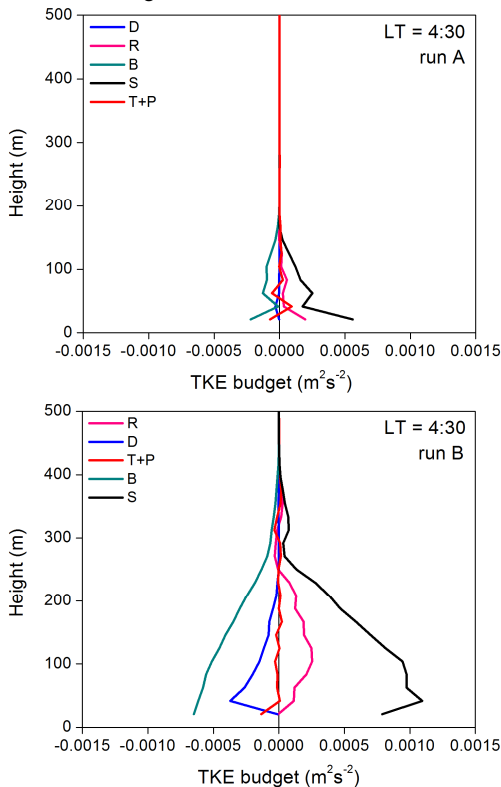


Fig. 17. Idem to figure 15 for 04:30 LT.

### 4.3. The effect of LLJ over the CO.

Figures 18, 19 and 20 show the time evolution of zonal component of wind, potential temperature and CO concentration simulated by LES model during nighttime for runs A and B.

The nighttime evolution of LLJ displayed in Fig. 18 are limited in the vertical to 1400 m in both simulations because it correspond to the height of residual mixed layer developed during the daytime. The time evolution of CO concentration displayed in Fig. 20 corresponds to simulation of SBL between 18:00 and 01:00 LT. This choice was made because the CO flux simulated by LES after 01:00 LT was not realistic (Fig. 14).

The nighttime evolution (Fig. 18) indicates that LLJ its maximum around 05:00 LT in both simulations, with intensity of  $7.2 \text{ ms}^{-1}$  for run A and  $14.7 \text{ ms}^{-1}$  for run B. Since the LLJ intensity depends on the momentum deficit in the end of convective period and the deficit of momentum is larger in the case of run B, the amplitude of wind in the inertial oscillation and LLJ intensity are higher in the run B.

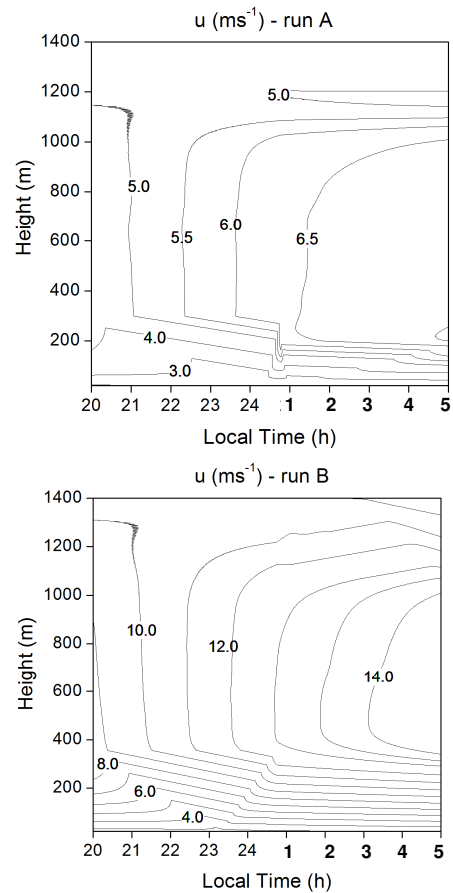


Fig.18. Nighttime evolution of the zonal component of the LLJ in the residual mixed layer.

On the other hand, the simulations indicate that the vertical position of the LLJ decreases progressively during nighttime for run A and run B.

In both cases the surface inversion layer deepens during the nighttime (Fig. 19). The thickness of the surface inversion layer varies from 120 m to about 180m in run A, and from 130 m to 310 m in B.

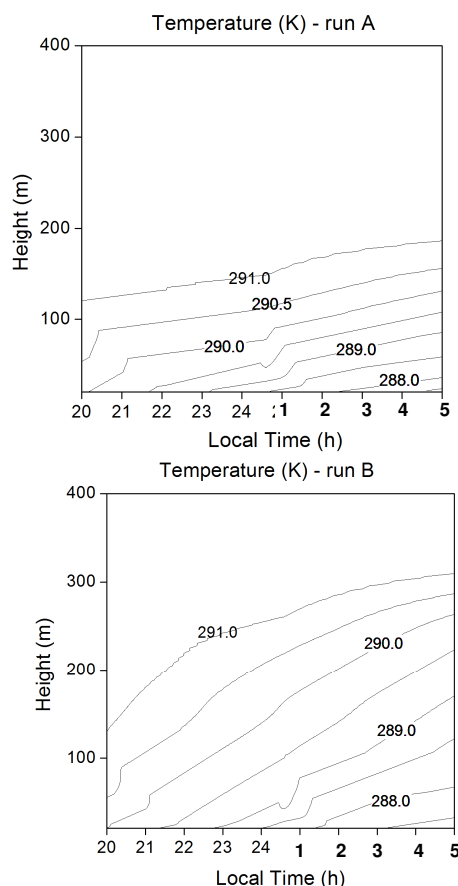


Fig. 19. Nighttime evolution of the surface inversion layer. LES results for run A and B.

Similar behavior is observed in the nighttime evolution of the CO concentration in the inversion layer (Fig. 20). The more intense LLJ generates a higher SBL and less intense surface inversion layer, this combination yields a higher concentration of CO to spread deeper in the atmosphere for a longer period of time.

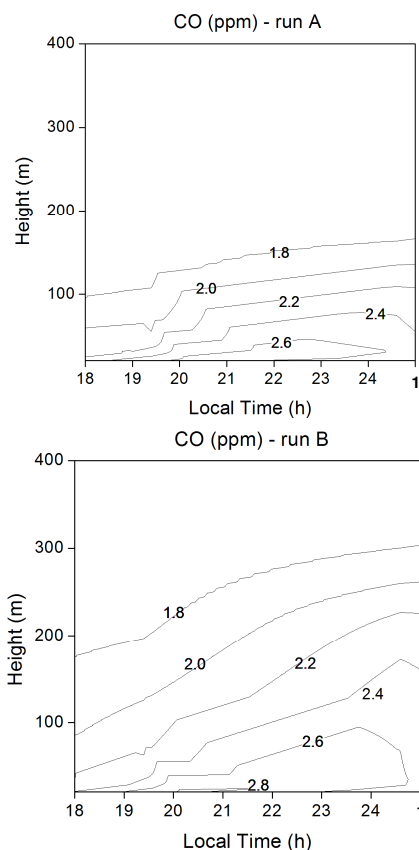


Fig.20. Nighttime evolution of CO concentration in the surface inversion layer. LES results for run A and B.

## 5. CONCLUSIONS

The main objective of this work is to investigate the role played by the inversion layer and LLJ on the CO time evolution at the surface in the city of São Paulo. Two numerical experiments, runs A and B, were carried using as external forcing geostrophic wind constant and equal to  $5 \text{ ms}^{-1}$  and  $10 \text{ ms}^{-1}$ . The PBL height is largest for run B in both convective (1240 m) and stable (275 m) periods. For run A, the PBL reaches 1088 m and 100 m for convective and stable conditions. During the daytime, the relative differences in the PBL height of runs A and B is about 20 % at most. During the nighttime, the PBL height differences are about 180%. Both simulations reproduced the diurnal evolution of heat flux observed in São Paulo during the winter ( $120\text{-}140 \text{ Wm}^{-2}$ ). The diurnal evolution of the simulated wind speed to run A compares well with observations in São Paulo during winter, indicates that external forcing associated with the prescribed geostrophic wind in this case is more realistic. During daytime, the simulated fluxes of CO, in both cases, match the estimated diurnal evolution of CO flux. Similar behavior occurs for the CO fluxes



until around midnight. After that, the simulated CO fluxes become unrealistic negative. The afternoon CO peak position is a little dislocated if compared with the CO values. This pattern, observed in both simulations, may be attributed to the fact that at afternoon, when convection becomes less intense, other non local effects, like horizontal advection of clean air associated to sea breeze penetration in São Paulo, become more important. The vertical distribution of TKE-equation components simulated by the model reproduced the expected features of PBL under convective conditions. At stable condition the molecular dissipation of TKE is small compared to the other relevant terms (shear production and thermal destruction). This rather unexpected result seems to be related to limitations in the sub-grid parameterizations and apparent lack of resolution of the grid used in the simulations carried here. The numerical simulations indicated that the CO concentration at the surface of Sao Paulo is mainly modulated by the inversion layer intensity, which depends on the intensity and position of the low level jet.

## 6. ACKNOWLEDGEMENTS

*The authors acknowledge the financial support provided by CNPq (Proc. No. 476807/2007-7 and 300561/91-1) and FAPESP (Proc. No. 2008/07532-0)*

## 7. BIBLIOGRAPHY

- Beare, R.J., McVean, M.K., Holtslag, A.A.M., Cuxart, J., Esau, I., Golaz, J.-C., Jimenez, M.A., Khairoutdinov, M., Kosovic, B., Lewellen, D., Lund, T.S., Lundquist, J.K., McCabe, A., Moene, A.F., Raasch, Y.N.S., Sullivan, P., 2006: An Intercomparison of Large-Eddy Simulations of the Stable Boundary Layer. *Boundary-Layer Meteorol.*, **118**, 247-272.
- Blackadar, A.K., 1957: Boundary Layer wind Maxima and their significance for the growth of nocturnal inversion. *Bull. Amer. Meteor. Soc.*, **38**, 283-290.
- Cederwall, R.T., 1995: Large-Eddy Simulation of the Development of Stably-Stratified Atmospheric Boundary Layers Over Cool Flat Surfaces. *11<sup>th</sup> Symposium on Boundary Layers and Turbulence*, Charlotte. North Caroline.
- CETESB Technical report, 2006: Technical report on air quality in the State of São Paulo - Environmental State Secretary, ISSN 0103-4103, São Paulo, Brazil, 137pp. (Available in Portuguese at <http://www.cetesb.sp.gov.br>).
- Codato, G., Oliveira, A.P., Soares, J., Marques Filho, E.P., and Rizza, U., 2008: Investigation of carbon monoxide in the city of São Paulo using large eddy simulation. *Proceedings of 15<sup>th</sup> Joint Conference on the Applications of Air Pollution Meteorology with the A&WMA*, 88<sup>th</sup> Annual Meeting, 20-24 January 2008, New Orleans, LO, USA.
- Cuxart, J. and Jiménez, M.A., 2007: Mixing Process in a Nocturnal Low-Level Jet: An LES Study. *J. Atmos. Res.*, **64**, 1666-1679.
- Galmarini, S. Beets, C. Duynkerke, P.G., Vilà-Guerau de Arellano, J., 1998: Stable Nocturnal Boundary Layers: A Comparison of One-Dimensional and Large-Eddy Simulation Models. *Boundary-Layer Meteorol.*, **88-2**, 1573-1472.
- Karipot, A., Leclerc, M.Y., Zhang, G., Lewin, K.F., Nagy, J., Hendrey, G.R., Starr, G., 2008: Influence of nocturnal low-level jet on turbulence structure and CO<sub>2</sub> flux measurements over a forest canopy. *J. Geophys. Res.*, **113**, DOI: 10.1029 /2007JD009149.
- Kosovic, B., Curry, J.A., 1999: A Large Eddy Simulation Study of a Quasi-Steady, Stably Stratified Atmospheric Boundary Layer. *J. Atmos. Sci.* **57** 1052-1068.
- Marques-Filho, E.P., Oliveira, A.P., Karam, H.A., Rizza, U., 2006: Pollutant transport in a convective boundary layer with LES. *Revista Brasileira de Geofísica*, **24(4)**, 547-557.
- Ferreira, M.J., 2009: Personal communication.
- Moeng, C.H., 1984: A Large Eddy Simulation Model for the Study of Planetary Boundary Layer Turbulence. *J. Atmos. Sci.* **41-13**: 2052-2062.
- Moeng, C.H., Wyngaard, J.C., 1988: Spectral Analysis of Large-Eddy-Simulations of the Convective Boundary Layer. *J. Atmos. Sci.*, **45-23**: 3573-3587.
- Saiki, E.M., Moeng, C-H., Sullivan, P.P., 2000: Large-Eddy Simulation of the Stably Stratified Planetary Boundary Layer. *Boundary-Layer Meteorol.* **95**, 1-30.
- Sorbjan, Z., Uliasz, M., 1999: Large-Eddy Simulation of air Pollution Dispersion in the Nocturnal Cloud-Topped Atmospheric Boundary Layer. *Boundary-Layer Meteorol.* **91(1)**, 145-157.
- Sullivan, P., McWilliams, J.C., Moeng, C.H., 1994: A subgrid-scale model for large-eddy simulation of planetary boundary-layer flows. *Boundary-Layer Meteorol.*, **71**, 247-276.
- van Dop, H., Axelsen, S., 2007: Large Eddy Simulation of the Stable Boundary-Layer: A retrospect to Nieuwstadt's Early Work. *Flow Turbulence Combust*, **79**, 235 – 249.
- Wang, L. and Pitsch, H., 2007: Large-Eddy Simulation on an industrial furnace with a cross-flow-jet combustion system. *Center for Turbulence Research, Annual Research Briefs*, 231-240.
- Wu, Y., and Raman, S., 1998: The summertime great plains low level jet and the effect of its origin on moisture transport, *Boundary-Layer Meteorol.*, **88**, 445– 46.